Infrared supercontinuum generated in concatenated InF_3 and As_2Se_3 fibers

Francis Théberge,[1], Nancy Bérubé,[1] Samuel Poulain,[2] Solenn Cozic,[2] Stéphane Châtigny,[3] Louis-Rafaël Robichaud,[3,4] Louis-Philippe Pleau,[4] Martin Bernier,[4] And Réal Vallée[4]

[1] Defence R&D Canada, Valcartier Centre, Québec, G3J 1X5, Canada
[2] Le Verre Fluoré, Campus KerLann, F-35170 Bruz, Brittany, France
[3] CorActive High-Tech Inc., Québec G2C 1S9, Canada
[4] Center for Optics, Photonics and Lasers (COPL), Université Laval, Québec G1V 0A6, Canada

Accepted for publication in *Optics Express*, May 2018

Abstract

We report on infrared supercontinuum (SC) generation through subsequent nonlinear propagation in concatenated step-index fluoride and As_2Se_3 fiber. These fibers were pumped by an all-fiber laser source based on an erbium amplifier followed by a thulium power amplifier. ZBLAN and InF_3 fibers were compared for the concatenated scheme. The broadest SC produced was achieved by optimizing the length of the InF_3 fiber. This arrangement allowed the generation of 200 mW infrared SC with high spectral flatness and spanning from 1.4 μm to 6.4 μm.

1. Introduction

High brightness broadband sources in the mid-infrared (MIR) atmospheric windows are needed for spectroscopy and metrology as well as defense applications [1–3]. Supercontinuum (SC) sources using fluorozirconate based fibers have reached watt level powers [4–9], but are restricted to wavelengths below ~4.2 μm when using long fibers. A wavelength extension of the SC above 5 μm is also possible when considering fluoroindate (InF_3) glass fibers [10–13]. The intrinsic fiber loss due to the multiphonon absorption edge in these fluoride-fibers is the main limitation on the long-wavelength side for SC generation. Emission beyond the multiphonon absorption edge can be achieved using small core and short lengths of fiber with high pump intensity [14–18]. Micron-sized suspended core or tapered fibers offer the possibility to adjust the fiber dispersion and enhance SC generation; however, these small core fibers cannot sustain high average laser powers. SC is also efficiently produced in chalcogenide (ChG) and tellurite fibers because both have very high nonlinear responses that are a few hundred times greater than fluoride fibers [19–22]. Moreover, the ChG fibers have multiphoton absorption edges at significantly longer wavelengths.

As shown in Table 1, there have been several demonstrations of infrared SC generation with ChG fibers [14,17,18,23–30] and some of them stand out by their output powers or their spectral bandwidths. The proper optical material for the conception of a ruggedized multi-watt SC source in the infrared is explored intensively by many research groups, and recent progresses in laser and fiber technologies indicate that such objectives should be reached in a near future. There are already impressive published results based on all-fiber laser sources (see Table 1); as for example, the generation of 565 mW over 1.3 octaves in As_2S_3 fiber [30]. In this case, the SC extension was limited by the S-H absorption band at 4.2 μm. A lot of effort has gone into producing high purity fibers in order to decrease the detrimental effects of contaminant absorption on SC broadening. Such improvements of the fluoride and ChG transmission allowed the generation of ultrabroadband SC in these fibers [4–18,23–29].

One promising development for producing powerful SC with a fiber-based laser source takes advantage of nonlinear propagation in concatenated fluoride and ChG fibers, which was first theoretically demonstrated in [31] by Kubat *et al*. and then experimentally proved [25,27,29]. The spectral and temporal compositions of continuum laser produced in fluoride fibers are critical for continued broadening in the following ChG fiber [27]. In order to make it efficient, the propagation loss in the ChG fibers must be low and its anomalous dispersion should overlap as most as possible with the SC produced by the fluoride fiber for further spectral broadening [31]. Recent work has succeeded in producing ~2.6 octave SC in concatenating three solid core fibers (ZBLAN, As_2S_3, and As_2Se_3) with an average output power of 139 mW, i.e. 417 mW on-time average power at 33% duty cycle [29]. Arsenic sulfide fiber was used as an intermediate fiber because the spectral expansion at the output of the ZBLAN fiber was not shifted at long enough wavelengths to pump efficiently the arsenic selenide fiber close to its zero-dispersion wavelength (ZDW). In our work, we present an alternative scheme where the ZBLAN fiber is replaced by an InF_3 fiber having a multiphonon absorption edge at longer wavelengths. This simplified scheme produced 2.2 octave SC generated in cascaded step-index InF_3 and As_2Se_3 fibers pumped by an all-fiber laser source. The average output power is 200 mW with high-spectral flatness and the SC extends from 1.4 μm to 6.4 μm. The recent production of high purity InF_3 and As_2Se_3 fibers has allowed these achievements and these fibers exhibit a MIR background loss of 0.02 dB/m and ~0.3 dB/m, respectively. In addition to their transmission, step-index InF_3 fibers exhibit favorable dispersion properties for SC generation when pumped within the thulium gain window, around 2 μm, and can sustain similar power densities than ZBLAN fibers [13].

2. Experimental setup

The SC distribution was measured with an f = 12.5 cm monochromator purged with dry nitrogen and equipped with a 300 lines/mm diffraction grating to provide a spectral resolution around 5 nm. A PbSe detector was used to measure the spectral fluence for the wavelength range from 1 μm to 4.8 μm, and a liquid nitrogen cooled HgCdTe detector from 2 μm to 13 μm. A set of long-pass filters were properly used to block any higher diffraction orders of the grating overlapping with the SC spectrum. The complete spectral response was calibrated with a blackbody radiation source (IR-508, Infrared Systems) for each combination of detector and long-pass filter.

The fiber-laser source used is shown in Fig. 1 and is based on a 1.55 μm pigtailed semiconductor laser diode delivering 50 ps pulses at 1 MHz repetition rate and amplified in an erbium-ytterbium doped (10 μm core) double-clad silica fiber pumped at 980 nm. Broadband spectrum ranging from 1.2 μm to 2.5 μm with 1.9 W of average power was produced in the 1.5 m long undoped silica fiber (8 μm core diameter) from the combiner spliced at the output of Er-Yb amplifier. The generated spectral components around 1.9 μm were preliminarily amplified in a Tm-doped single-clad silica fiber (see SCF-Tm-8/125 μm in Fig. 1) and then spectrally filtered with a fiber isolator. The spectral components around 1.9 μm were further amplified in a 10 μm core diameter thulium (Tm) doped double-clad silica fiber pumped at 791 nm. The spectral distribution of the amplified laser pulse is shown in Fig. 2(a) (green dash-dot line) and the 2.03 W output power was butt-coupled using flat cleaves into a ZBLAN or InF_3 fiber and both fluoride fibers were wound on a spool having a radius of 10 cm.

The butt-coupling efficiencies between the Tm-amplifier and the fluoride fibers were 56% for the ZBLAN fiber and to 60% for the InF_3 fiber. The output continuum from the fluoride fiber was then coupled into the arsenic selenide fiber (core/clad material: $As_{35.6}Se_{64.4}/As_{35}Se_{65}$) with a black-diamond lens having an anti-reflection coating for the 2-5 μm range (f = 5.95 mm, NA = 0.56). The alignment of the ChG fiber was optimized by monitoring the SC output power and the spectral extension. Different combinations of ZBLAN, InF_3 and ChG fibers have been tested and are discussed below. Table 2 summarizes the main parameters of these fibers. For reference, their measured attenuations are shown in Fig. 2(b) and the dispersion of the fundamental mode for these fibers is shown in Fig. 2(c) and was calculated with commercial software (Mode Solutions, Lumerical Inc [32].). The computation of the ChG and ZBLAN dispersions are based on the Sellmeier equation with coefficients from Dantanarayana *et al*. and Zhang *et al*. [33,34], respectively. For InF_3, the index of refraction was measured from a bulk sample with an infrared ellipsometer. The calculated dispersion for the InF_3 fiber was confirmed for wavelengths between 2.3 μm and 2.5 μm by measuring the dispersion of an 81-cm long InF_3 fiber sample in a white-light interferometer.

3. Results and discussion

Among the fiber combinations of ZBLAN-As_2Se_3 or InF_3-As_2Se_3, the most efficient in terms of spectral broadening and output power is shown in Fig. 2(a), and was obtained with an 8 m InF_3 fiber concatenated with a 9 m of As_2Se_3 fiber. For comparison, the SC obtained by replacing the InF_3 fiber by an 8 m ZBLAN fiber is also shown in Fig. 2(a). The SC obtained by pumping the ChG fiber with the InF_3 continuum spans from 1.4 to 6.4 μm (2.2 octaves), while the SC generated with the ZBLAN continuum produced a narrower SC (1.9 octaves) with a similar output power of 206 mW.

The dynamics of the SC generation in optical fibers is well known. When the fiber is pumped with picosecond pulses in the anomalous dispersion region, as for the cases of fluoride fibers used in this work, modulation instability (MI) and self-phase modulation (SPM) are the main phenomena in the first step of SC generation. After a certain propagation length, this MI leads to the temporal breakup of injected pulses into a distributed spectrum of many shorter subpulses, which then propagate through the fiber. Subsequently, each subpulse undergoes further spectral broadening through MI, SPM and Raman-induced frequency red-shift [35]. In opposite, the ChG fiber exhibits all-normal dispersion up to a wavelength of 8.7 μm. Therefore, the continuum lasers from the InF3 or ZBLAN fibers injected into the ChG fiber broaden mainly through SPM or Raman-induced frequency red-shift. One of these two mechanisms is favored depending if the pulsewidth of each subpulses (solitons) injected into the ChG fiber is shorter or longer than picosecond timescale, respectively [35].

As shown in Fig. 2(a), the output from the ZBLAN fiber produced brighter signal in its continuum around 4 μm than the InF_3 fiber, but the ZBLAN multiphonon absorption edge limited the continuum extension into the MIR. In contrast, the lower dispersion of the InF_3 fiber [Fig. 2(c)] around the pump wavelengths (between 1.8 to 2.6 μm) minimizes initially the pulse stretching, but once the spectral broadening extends between 3 μm and 5 μm, both ZBLAN and InF_3 dispersions are similar for these spectral components. These factors improve the spectral and temporal profile of the InF_3 continuum and inject more intense solitons in the MIR wavelengths which result in broader SC in the following ChG fiber. It is important to note that the temporal distribution of the continuum produced by ZBLAN and InF_3 fibers could not be measured with spectrally resolved autocorrelation techniques because their continua were too broad for complete phase-matching of the second-harmonic generation signal.

However, in order to investigate the impact of the temporal and spectral distribution of the continuum laser injected into the ChG fiber, Fig. 3(b) presents the output SC from a 9 m ChG fiber concatenated to three different lengths of InF_3 fiber (continuum lasers shown in Fig. 3(a)). As expected, the longest InF_3 fiber (12 m), produced the broadest continuum laser (orange line in Fig. 3(a)). However, this continuum laser injected into the 9-m ChG fiber produced the narrowest SC as presented in Fig. 3(b). This indicates that the 12-m InF_3 fiber produced broader spectrum, but less intense MIR subpulses to pump the following ChG fiber. The lower efficiency of the continuum laser produced by the 12-m long InF_3 fiber is probably due to the temporal broadening of the MIR subpulses propagating in the longer InF_3 fiber, which reduced their intensities and the nonlinear effects in the following ChG fiber. In contrast, the use of shorter InF_3 fiber (3 m long) produced a continuum laser that was ~500 nm narrower than for the 12-m long InF_3 fiber. Notwithstanding, the continuum laser from the 3-m long InF_3 fiber produced a SC at the output of the ChG fiber that was slightly larger by ~150 nm than that using the longest InF_3 fiber. In terms of spectral bandwidth at the output of the ChG fiber, the optimum InF_3 fiber length to pump the ChG fiber was around 8 m long, where the MIR subpulse intensities and their spectral extensions at the InF_3 fiber output are the best compromises to pump the following ChG fiber in its normal dispersion regime.

The impact of the ChG fiber length on the SC distribution is shown in Fig. 4 for the same injection of continuum laser (890 mW) from the 8-m long InF_3 fiber. The spectral distribution of the continuum laser (red curve) is shown again in Fig. 4 for reference. We clearly see that the MIR extension increases from ~4.5 μm to ~5.7 μm within the first meters of propagation in the ChG fiber. As expected, further increases to the ChG fiber length prolong the MIR SC extension, but at a slower rate. Since the spectral broadening was asymmetric and accentuated towards longer wavelengths, it can be inferred that Raman soliton self-frequency shift was a dominant process for the supercontinuum generation in the ChG fibers. On the other hand, increasing the length of the ChG fiber decreases the total SC output power due mainly to the ChG MIR background loss ranging around ~0.3 dB/m. Therefore, increasing more the ChG fiber length can increase the spectral broadening, but at the cost of a rapid decrease of the SC output power [Fig. 5] [25]. The optimum length in terms of spectral broadening and output power was experimentally observed for 9-m long ChG fiber.

Different lengths and combinations of ZBLAN, InF_3 and ChG fibers have been tested and both their 20-dB spectral bandwidths and output powers are presented in Fig. 5 for the maximum Tm amplifier output power, i.e. 2.03 W. The concatenated scheme that produced the broadest SC used 8 m of InF_3 fiber as shown previously in Figs. 2(a) and 3(b). When using ZBLAN fiber, the optimum length was also around 8 m, but the resulting SC was narrower [Fig. 5(a)]. For this specific energy and pulsewidth at the output of the Tm amplifier (2 μJ, ~50 ps), the use of shorter or longer ZBLAN/InF_3 fibers reduced the spectral broadening at the output of the ChG fiber because the spectral and temporal distribution of the continuum laser from the fluoride fiber was less efficient for spectral broadening in the normal dispersion regime of the following ChG fiber. On the other hand, for all results presented in Fig. 5(a), the use of InF_3 fibers (blue curves) produced broader SC at the output of the ChG fiber than by using initially a ZBLAN fiber (red curves). Finally, as shown in Fig. 5(b), the SC average power at the output of the ChG fiber was similar for both concatenated schemes using initially a ZBLAN or InF_3 fiber. The use of longer ChG fiber increases the spectral broadening, but significantly decreases the SC output power because the MIR background loss of the ChG fiber is about 10 times higher than for the fluoride fiber [Figs. 2(b) and 5(b)].

The use of a smaller core step-index As_2Se_3 fiber (14.6 μm core diameter, NA = 0.21) has also been tested in order to potentially increase the laser intensity in its core, to shift the ChG ZDW closer to the continuum extension of the fluoride fibers, and therefore enhance the spectral broadening. However, the smaller ChG fiber core has a higher MIR background loss and the decrease of its core diameter slightly reduced also the coupling of the MIR continuum from the fluoride fiber. Consequently, the spectral broadening was lower in our experiment with the smaller ChG fiber core (14.6 μm, NA = 0.21) than for the larger diameter ChG fiber core (18 μm, NA = 0.22).

4. Conclusions

In summary, we have presented the first demonstration of 2.2 octave SC generated in concatenated step-index InF_3 and As_2Se_3 fibers pumped by an all-fiber laser source. The average output power reached 200 mW with high-spectral flatness and the SC was extended from 1.4 μm to 6.4 μm. The use of InF_3 fiber instead of ZBLAN fiber in concatenated scheme clearly showed advantages on the spectral broadening mainly because of its longer multiphonon absorption edge. In addition to their wider transmission, step-index InF_3 fibers exhibit favorable dispersion properties for SC generation when pumped within the thulium gain window, around 2 μm, and can sustain similar power densities than ZBLAN fibers [13]. Small core arsenic selenide fibers also recently were proven to sustain up to Watt-level SC output power around 2 μm [36], which demonstrates their potential robustness. Increasing the laser repetition rate, with similar laser pulse parameters than in our work, is a direct way to increase the SC output power from the fluoride and ChG fibers. However, the use of long ChG fiber in our concatenated scheme was an important factor limiting the output power and the SC extension due to ChG fiber loss. Consequently, an optimization of the Tm amplifier dispersion could produce shorter laser pulses allowing the use of shorter fluoride and ChG fibers; and therefore, further extend the SC and increase the output power. Finally, and as demonstrated in [37] by Guo *et al.*, the use of larger numerical aperture As_2Se_3 fibers should also have significant effects on the long wavelength extension of the generated SC by reducing the mode field diameter and increasing the nonlinearity.

Funding

Defence R & D Canada Program and the Natural Sciences and Engineering Research Council of Canada (NSERC) (IRCPJ469414-13).

Acknowledgments

The authors acknowledge the technical support of Pascal Duchesne and want to thank Pierre Mathieu and Denis Vincent for their fruitful discussions.

References

1. S. Dupont, C. Petersen, J. Thøgersen, C. Agger, O. Bang, and S. R. Keiding, "IR microscopy utilizing intense supercontinuum light source," Opt. Express 20(5), 4887–4892 (2012).
2. S. Lambert-Girard, M. Allard, M. Piché, and F. Babin, "Differential optical absorption spectroscopy lidar for mid-infrared gaseous measurements," Appl. Opt. 54(7), 1647–1656 (2015).
3. M. N. Islam, M. J. Freeman, L. M. Peterson, K. Ke, A. Ifarraguerri, C. Bailey, F. Baxley, M. Wager, A. Absi, J. Leonard, H. Baker, and M. Rucci, "Field tests for round-trip imaging at a 1.4 km distance with change detection and ranging using a short-wave infrared supercontinuum laser," Appl. Opt. 55(7), 1584–1602 (2016).
4. O. P. Kulkarni, V. V. Alexander, M. Kumar, M. J. Freeman, M. N. Islam, F. Terry, Jr., M. Neelakandan, and A. Chan, "Supercontinuum generation from ~1.9 to 4.5 μm in ZBLAN fiber with high average power generation beyond 3.8 μm using a thulium-doped fiber amplifier," J. Opt. Soc. Am. B 28(10), 2486–2498 (2011).
5. J. Swiderski and M. Michalska, "High-power supercontinuum generation in a ZBLAN fiber with very efficient power distribution toward the mid-infrared," Opt. Lett. 39(4), 910–913 (2014).
6. J. Swiderski, M. Michalska, C. Kieleck, M. Eichhorn, and G. Mazé, "High Power Supercontinuum Generation in Fluoride Fibers Pumped by 2 μm Pulses," IEEE Photonics Technol. Lett. 26(2), 150–153 (2014).
7. Z. Zheng, D. Ouyang, J. Zhao, M. Liu, S. Ruan, P. Yan, and J. Wang, "Scaling all-fiber mid-infrared supercontinuum up to 10 W-level based on thermal-spliced silica fiber and ZBLAN fiber," Photon. Res. 4(4), 135–139 (2016).
8. K. Yin, B. Zhang, L. Yang, and J. Hou, "15.2 W spectrally flat all-fiber supercontinuum laser source with >1 W power beyond 3.8 μm," Opt. Lett. 42(12), 2334–2337 (2017).
9. C. Kneis, B. Donelan, I. Manek-Hönninger, T. Robin, B. Cadier, M. Eichhorn, and C. Kieleck, "High-peak-power single-oscillator actively Q-switched mode-locked Tm3+-doped fiber laser and its application for high-average output power mid-IR supercontinuum generation in a ZBLAN fiber," Opt. Lett. 41(11), 2545–2548 (2016).
10. F. Théberge, J.-F. Daigle, D. Vincent, P. Mathieu, J. Fortin, B. E. Schmidt, N. Thiré, and F. Légaré, "Mid-infrared supercontinuum generation in fluoroindate fiber," Opt. Lett. 38(22), 4683–4685 (2013).
11. J.-C. Gauthier, V. Fortin, J.-Y. Carrée, S. Poulain, M. Poulain, R. Vallée, and M. Bernier, "Mid-IR supercontinuum from 2.4 to 5.4 μm in a low-loss fluoroindate fiber," Opt. Lett. 41(8), 1756–1759 (2016).
12. M. Michalska, J. Mikolajczyk, J. Wojtas, and J. Swiderski, "Mid-infrared, super-flat, supercontinuum generation covering the 2-5 μm spectral band using a fluoroindate fibre pumped with picosecond pulses," Sci. Rep. 6(1), 39138 (2016).
13. F. Théberge, N. Bérubé, S. Poulain, S. Cozic, L.-R. Robichaud, M. Bernier, and R. Vallée, "Watt-level and spectrally flat mid-infrared supercontinuum in fluoroindate fibers," Photon. Res. (accepted).
14. H. Ou, S. Dai, P. Zhang, Z. Liu, X. Wang, F. Chen, H. Xu, B. Luo, Y. Huang, and R. Wang, "Ultrabroad supercontinuum generated from a highly nonlinear Ge-Sb-Se fiber," Opt. Lett. 41(14), 3201–3204 (2016).
15. R. R. Gattass, L. Brandon Shaw, and J. S. Sanghera, "Microchip laser mid-infrared supercontinuum laser source based on an As2Se3 fiber," Opt. Lett. 39(12), 3418–3420 (2014).
16. O. Mouawad, J. Picot-Clémente, F. Amrani, C. Strutynski, J. Fatome, B. Kibler, F. Désévédavy, G. Gadret, J.-C. Jules, D. Deng, Y. Ohishi, and F. Smektala, "Multioctave midinfrared supercontinuum generation in suspended-core chalcogenide fibers," Opt. Lett. 39(9), 2684–2687 (2014).
17. C. R. Petersen, U. Møller, I. Kubat, B. Zhou, S. Dupont, J. Ramsay, T. Benson, S. Sujecki, N. Abdel-Moneim, Z. Tang, D. Furniss, A. Seddon, and O. Bang, "Mid-infrared supercontinuum covering the 1.4–13.3 μm molecular fingerprint region using ultra-high NA chalcogenide step-index fibre," Nat. Photonics 8(11), 830–834 (2014).
18. T. Cheng, K. Nagasaka, T. H. Tuan, X. Xue, M. Matsumoto, H. Tezuka, T. Suzuki, and Y. Ohishi, "Mid-infrared supercontinuum generation spanning 2.0 to 15.1 μm in a chalcogenide step-index fiber," Opt. Lett. 41(9), 2117–2120 (2016).
19. K. Yin, B. Zhang, J. Yao, Z. Cai, G. Liu, and J. Hou, "Toward High-Power All-Fiber 2-5 μm Supercontinuum Generation in Chalcogenide Step-Index Fiber," J. Lightwave Technol. 35(20), 4535–4539 (2017).
20. Z. Zhao, B. Wu, X. Wang, Z. Pan, Z. Liu, P. Zhang, X. Shen, Q. Nie, S. Dai, and R. Wang, "Mid-infrared supercontinuum covering 2.0-16 μm in a low-loss telluride single-mode fiber," Laser Photonics Rev. 11(2), 1700005 (2017).
21. N. Tolstik, E. Sorokin, V. Kalashnikov, and I. Sorokina, "Soliton delivery of mid-IR femtosecond pulses with ZBLAN fiber," Opt. Mater. Express 2(11), 1580–1587 (2012).
22. J. S. Sanghera, I. D. Aggarwal, L. B. Shaw, C. M. Florea, P. Pureza, V. Q. Nguyen, F. Kung, and I. D. Aggarwal, "Nonlinear properties of chalcogenide glass fibers," J. Opto-Elect. Adv. Mater. 8, 2148–2155 (2006).
23. X. Han, C. You, S. Dai, P. Zhang, Y. Wang, F. Guo, D. Xu, B. Luo, P. Xu, and X. Wang, "Mid-infrared supercontinuum generation in a three-hole Ge20Sb15Se65 chalcogenide suspended-core fiber," Opt. Fiber Technol. 34, 74–79 (2017).

24. F. Théberge, N. Thiré, J.-F. Daigle, P. Mathieu, B. E. Schmidt, Y. Messaddeq, R. Vallée, and F. Légaré, "Multioctave infrared supercontinuum generation in large-core As2S3 fibers," Opt. Lett. 39(22), 6474–6477 (2014).

25. L.-R. Robichaud, V. Fortin, J.-C. Gauthier, S. Châtigny, J.-F. Couillard, J.-L. Delarosbil, R. Vallée, and M. Bernier, "Compact 3-8 μm supercontinuum generation in a low-loss As2Se3 step-index fiber," Opt. Lett. 41(20), 4605–4608 (2016).

26. D. Deng, L. Liu, T. H. Tuan, Y. Kanou, M. Matsumoto, H. Tezuka, T. Suzuki, and Y. Ohishi, "Mid-infrared supercontinuum covering 3–10μm using a As2Se3 core and As2S5 cladding step-index chalcogenide fiber," J. Cer. Soc. Jpn. 124, 103–105 (2016).

27. C. R. Petersen, P. M. Moselund, C. Petersen, U. Møller, and O. Bang, "Spectral-temporal composition matters when cascading supercontinua into the mid-infrared," Opt. Express 24(2), 749–758 (2016).

28. D. D. Hudson, S. Antipov, L. Li, I. Alamgir, T. Hu, M. El Amaraoui, Y. Messaddeq, M. Rochette, S. D. Jackson, and A. Fuerbach, "Toward all-fiber supercontinuum spanning the mid-infrared," Optica 4(10), 1163–1166 (2017).

29. R. A. Martinez, G. Plant, K. Guo, B. Janiszewski, M. J. Freeman, R. L. Maynard, M. N. Islam, F. L. Terry, O. Alvarez, F. Chenard, R. Bedford, R. Gibson, and A. I. Ifarraguerri, "Mid-infrared supercontinuum generation from 1.6 to >11 μm using concatenated step-index fluoride and chalcogenide fibers," Opt. Lett. 43(2), 296–299 (2018).

30. R. R. Gattass, L. B. Shaw, V. Q. Nguyen, P. C. Pureza, I. D. Aggarwal, and J. S. Sanghera, "All-fiber chalcogenide-based mid-infrared supercontinuum source," Opt. Fib. Technol. 18(5), 345–348 (2012).

31. I. Kubat, C. R. Petersen, U. V. Møller, A. Seddon, T. Benson, L. Brilland, D. Méchin, P. M. Moselund, and O. Bang, "Thulium pumped mid-infrared 0.9-9μm supercontinuum generation in concatenated fluoride and chalcogenide glass fibers," Opt. Express 22(4), 3959–3967 (2014).

32. www.lumerical.com.

33. H. G. Dantanarayana, N. Abdel-Moneim, Z. Tang, L. Sojka, S. Sujecki, D. Furniss, A. B. Seddon, I. Kubat, O. Bang, and T. M. Benson, "Refractive index dispersion of chalcogenide glasses for ultra-high numerical-aperture fiber for mid-infrared supercontinuum generation," Opt. Mater. Express 4(7), 1444–1455 (2014).

34. L. Zhang, F. Gan, and P. Wang, "Evaluation of refractive-index and material dispersion in fluoride glasses," Appl. Opt. 33(1), 50–56 (1994).

35. G. Genty, S. Coen, and J. M. Dudley, "Fiber supercontinuum sources (Invited)," J. Opt. Soc. Am. B 24(8), 1771–1785 (2007).

36. Y. Tang, F. Li, and J. Xu, "Watt-level supercontinuum generation in As2Se3 fibers pumped by a 2-micron random fiber laser," Laser Phys. 26(5), 055402 (2016).

37. K. Guo, R. A. Martinez, G. Plant, L. Maksymiuk, B. Janiszewski, M. J. Freeman, R. L. Maynard, M. N. Islam, F.

38. Terry, R. Bedford, R. Gibson, F. Chenard, S. Châtigny, and A. I. Ifarraguerri, "Generation of near-diffraction-limited, high-power supercontinuum from 1.57 μm to 12 μm with cascaded fluoride and chalcogenide fibers," Appl. Opt. 57(10), 2519–2532 (2018).

Table 1. Characteristics of Chalcogenide Fiber-Based SC Laser Sources[a]

Reference	Short description	20 dB spectral bandwidth	Average power (mW)
23	150 fs OPA (λ_c = 3.3 μm) in suspended core Ge-Sb-Se fiber	1.3 octaves	0.1
24	130 fs OPA (λ_c = 4.56 μm) in step-index As_2S_3 fiber	2.2 octaves	0.1
14	150 fs OPA (λ_c = 6.0 μm) in step-index Ge-Sb-Se fiber	1.7 octaves	0.1
17	100 fs OPA (λ_c = 6.3 μm) in step-index As_2Se_3 fiber	3.2 octaves	1
25	Er-ZBLAN fiber amplifier in concatenated ZBLAN & As_2Se_3 fibers	1.2 octaves	1.5
26	85 fs OPA (λ_c ~7 μm) in As_2Se_3 core and As_2S_5 clad fiber	1.7 octaves	<3
18	170 fs OPA (λ_c ~9.8 μm) in As_2Se_3 fiber	2.9 octaves	<3
27	Tm-doped silica amplifiers in concatenated ZBLAN & As_2Se_3 fibers	1.6 octaves	6.5
28	Ho-Pr ZBLAN fiber amplifier in As_2Se_3/As_2S_3 tapered fiber	2.0 octaves	30
29	Tm-doped amplifiers in concatenated ZBLAN, As_2S_3 & As_2Se_3 fibers	2.5 octaves	139
This work	Tm-doped amplifiers in concatenated 8 m InF_3 & 9 m As_2Se_3 fibers	2.0 octaves	200
This work	Tm-doped amplifiers in concatenated 8 m InF_3 & 3 m As_2Se_3 fibers	1.75 octaves	360
30	Tm-doped silica amplifier injected in As_2S_3	1.3 octaves	565

[a]OPA, optical parametric amplifier; λ_c, laser central wavelength; Er, erbium; Tm, thulium; Ho, holmium; Pr, praseodymium

Table 2. Fiber Parameters Summary[b]

Parameter	ZBLAN	InF_3	As_2Se_3
Core diameter (μm)	8.5	9.5	18
Clad diameter (μm)	125	100	170
ZDW (μm)	1.6	1.9	8.7
NA	0.23	0.3	0.22
Cut-off (μm)	2.4	3.7	5.2
Manufacturer	LVF	LVF	CorActive

[b] ZDW, zero dispersion wavelength; LVF, Le Verre Fluoré

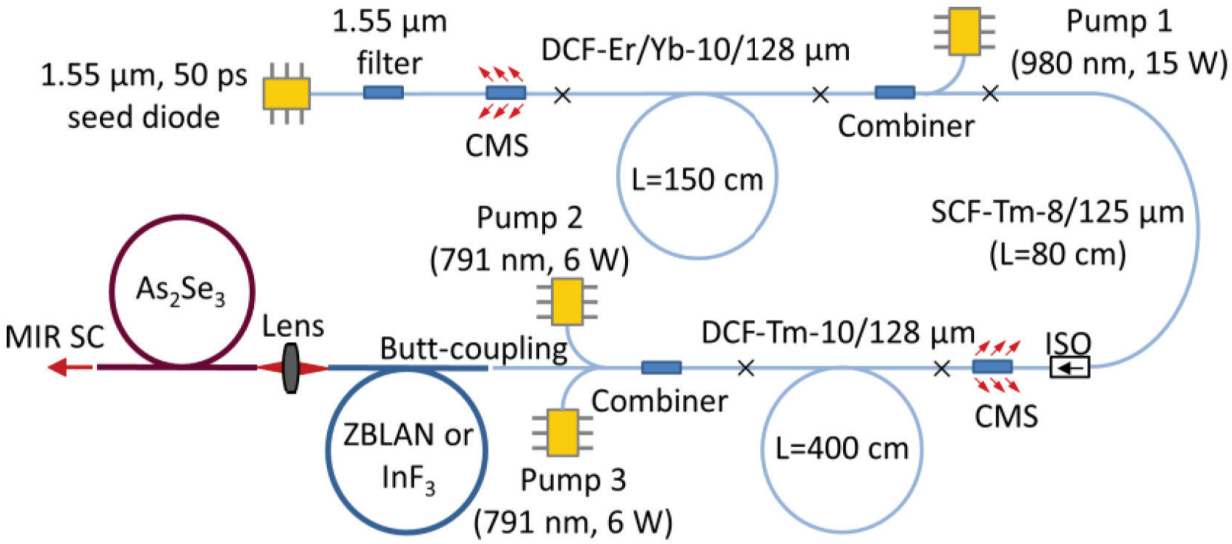

Fig. 1. Experimental setup of the MIR SC fiber source. CMS, cladding mode stripper; DCF, double-clad fiber, SCF, single-clad fiber, ISO, 1.9 µm optical isolator, L, fiber length.

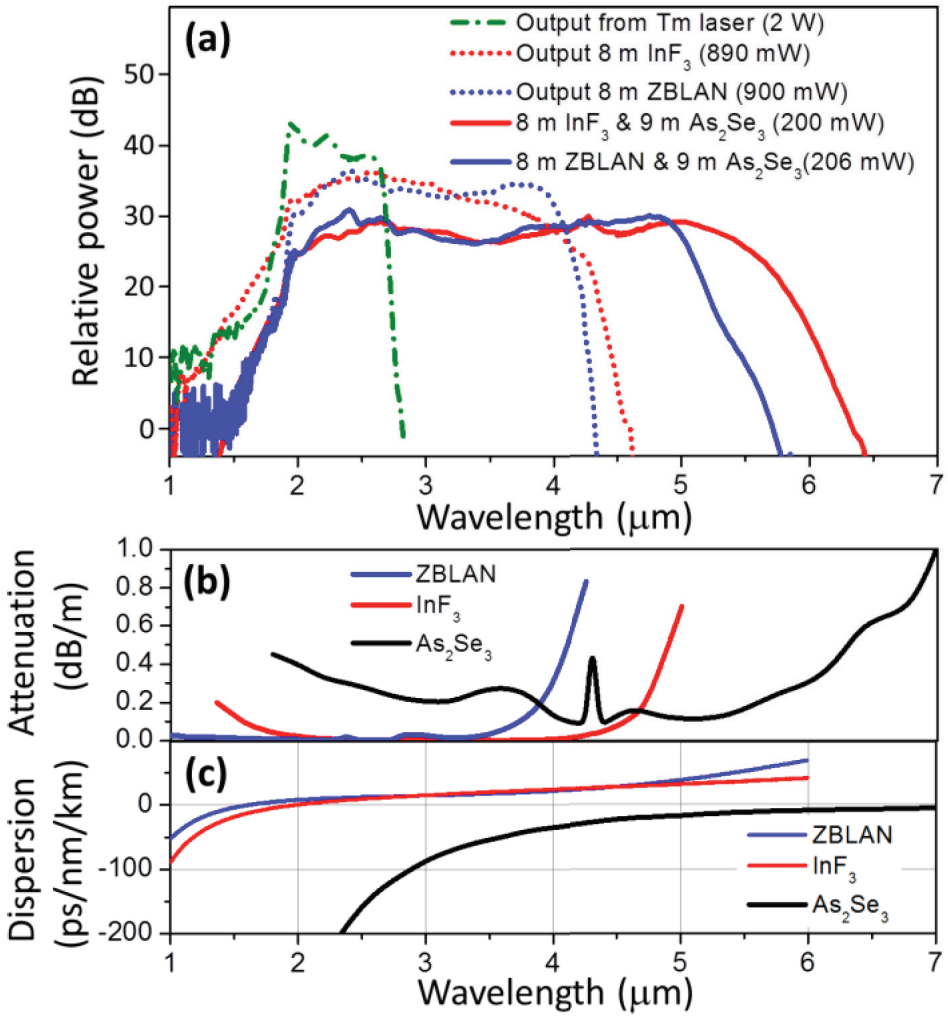

Fig. 2. (a) Spectral distribution of the Tm amplifier (green dash-dot line) injected into fluoride fibers. The continuum from the 8-m ZBLAN or 8-m InF_3 fibers are shown by the blue dashed and the red dashed lines, respectively. The output SC from the 9-m ChG fiber pumped by the continuum of the InF_3 (red line) or by the continuum of the ZBLAN (blue line) fibers are also presented. (b) Measured spectral attenuation of the ZBLAN, InF_3 and ChG fibers using standard cut-back procedure with a Fourier-transform infrared spectrometer. The measurements were smoothed over 50 nm bandwidth. (c) Calculated dispersion of the ZBLAN, InF_3 and ChG fibers used.

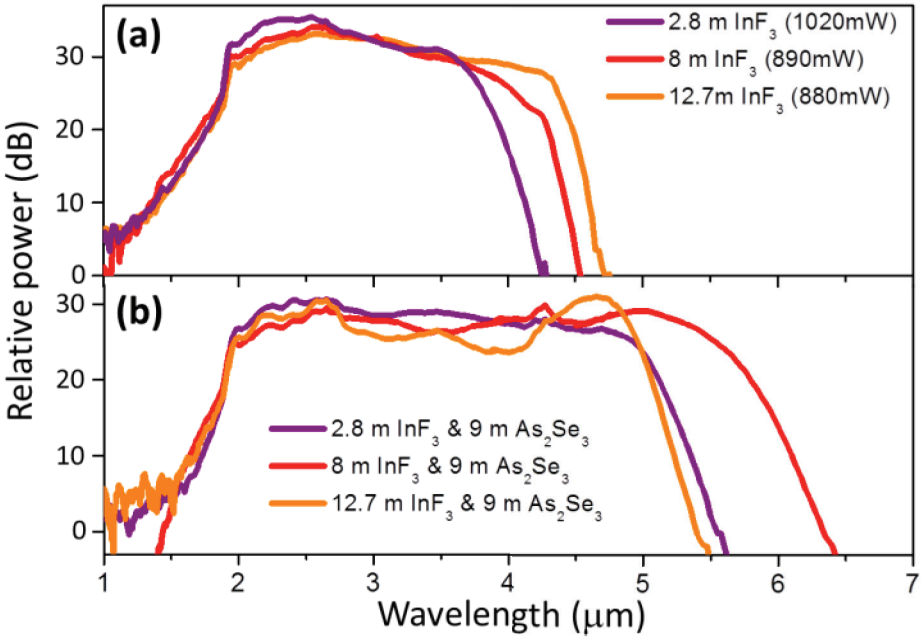

Fig. 3. (a) Spectral distribution at the output of the InF_3 fiber for three different lengths of fiber. The laser power from the Tm amplifier and injected into the InF_3 fibers was fixed to 2.03 W for the three cases presented and their output powers are indicated in parenthesis. (b) The output SC from the 9-m ChG fiber pumped by the continuum from three different lengths of InF_3 fiber.

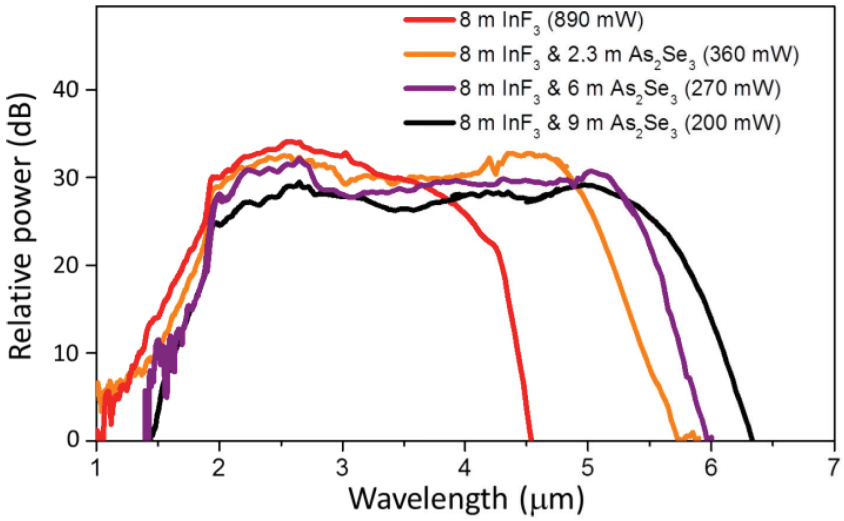

Fig. 4. Spectral distribution at the output of the ChG fiber for three different ChG fiber lengths. The continuum laser power from the 8-m InF_3 fiber injected into the three different ChG fiber lengths was fixed to 890 mW (spectral distribution shown by the red line).

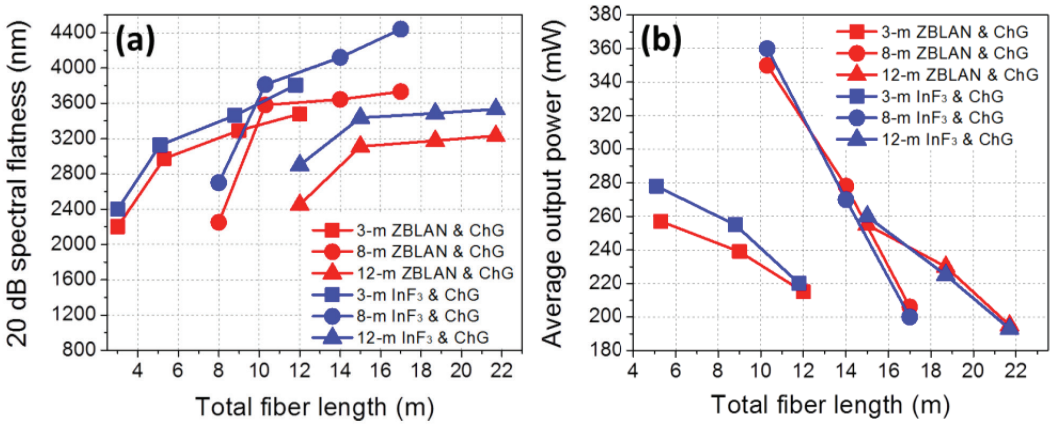

Fig. 5. (a) 20 dB spectral flatness and (b) average output power of the SC produced for different combinations of fluoride and ChG fibers as a function of their total lengths. The total fiber length on the horizontal axis corresponds to the sum of the fluoride and ChG fiber lengths.